

# The Inverse Mach Reflection

K. Takayama\*

Tohoku University, Sendai, Japan  
and

G. Ben-Dor†

Ben-Gurion University of the Negev, Beer Sheva, Israel

**A particular type of Mach reflection—the inverse Mach reflection—is investigated both experimentally and theoretically. It is shown that the inverse Mach reflection is of a fundamental type in truly unsteady flows. The special characteristics of the inverse Mach reflection as well as the differences between it and the well-known stationary and direct Mach reflections are discussed. A unique property of the inverse Mach reflection, i.e., its reflection from a solid surface, is revealed experimentally and explained analytically using shock polars. The importance of this research lies in the fact that the inverse Mach reflection plays a significant role in the Mach reflection phenomenon in truly unsteady flows to which many such phenomena in nature belong.**

## Introduction

**T**HE Mach reflection—a three-shock wave configuration—was first discovered by E. Mach<sup>1</sup> more than 100 years ago. Since the Mach reflection occurs in many flowfields having shock waves, it has drawn special attention in the past few decades. Probably the most significant evidence of its importance is the fact that a special meeting entitled “The Mach Reflection Symposium” has been held annually since 1981. (Details concerning these meetings are available from the authors.)

The Mach reflection phenomenon can be found in a variety of flowfields—e.g., planar shock wave interactions with straight and curved wedges, blast wave phenomena, underwater explosions, detonation waves, and shock wave propagation in channels and tubes.

As will be shown subsequently, the Mach reflection configuration can be divided into three categories: direct, stationary, and inverse. While the direct and stationary Mach reflections are well known and quite intensively discussed in the open literature, the inverse Mach reflection is almost unmentioned and untreated. This is probably due to the fact that, in most phenomena in which Mach reflections occur, it is usually direct and/or stationary Mach reflections that take place. Nevertheless, recent investigations have indicated that the inverse Mach reflection plays a significant role in the transition from Mach to regular reflection in truly unsteady flows.

Probably the first detailed description of the inverse Mach reflection was given by Courant and Friedrichs,<sup>3</sup> who called it inverted Mach reflection. Oppenheim, et al.<sup>4</sup> mentioned it as one of the possible shock interactions in their study of detonation waves.

The aim of the present study is to reveal this particular type of Mach reflection and to establish its physical characteristics and behavior.

## Present Study

As mentioned earlier, the Mach reflection phenomenon can be divided into three different types. These types are schematically shown in Fig. 1. Each Mach reflection configuration consists of four discontinuities (three shock waves and one slipstream): incident shock wave *I*, reflected shock wave *R*, Mach stem *M*, and slipstream *S*. The point of confluence (the triple point) is designated by *T*. The triple-point

trajectories are shown by dashed lines. Using Fig. 1 one can define:

- 1) Direct Mach reflection as a three-shock confluence in which the triple point moves away from the reflecting wedge.
- 2) Stationary Mach reflection as a three-shock confluence in which the triple point moves parallel to the reflecting wedge.
- 3) Inverse Mach reflection as a three-shock confluence in which the triple point moves toward the reflecting wedge.

Using the following notation, one can put these definitions into a simple mathematical form. Let us define the length of the Mach stem as  $\lambda$  and the distance it travels along the wedge as  $S$ . Consequently,

$$\begin{aligned} \frac{d\lambda}{dS} &> 0 && \text{direct Mach reflection} \\ &= 0 && \text{stationary Mach reflection} \\ &< 0 && \text{inverse Mach reflection} \end{aligned}$$

There is yet another way to differentiate between these three types of Mach reflections. Consider Fig. 2 in which direct and inverse Mach reflections are shown schematically. For clarity, the reflected shock wave *R* and the slipstream *S* are omitted. Attaching a frame of reference to the triple point *T* and defining the angle of incidence between the oncoming flow and the incident shock wave *I* as  $\phi_0$  yields, for a direct Mach reflection (Fig. 2a),

$$\theta_w + \chi = 90 \text{ deg} - \phi_0 \quad (1)$$

and for an inverse Mach reflection (Fig. 2b)

$$\theta_w - \chi = 90 \text{ deg} - \phi_0 \quad (2)$$

where  $\chi$  is the angle between the reflecting wedge surface and the triple-point trajectory. Equation (2) can be rewritten as

$$\theta_w + (-\chi) = 90 \text{ deg} - \phi_0 \quad (3)$$

Thus, Eqs. (1) and (3) indicate that the three types of Mach reflection can be differentiated by the value of the triple-point trajectory angle  $\chi$ , i.e.,

$$\begin{aligned} \chi &> 0 && \text{direct Mach reflection} \\ &= 0 && \text{stationary Mach reflection} \\ &< 0 && \text{inverse Mach reflection} \end{aligned}$$

Received Jan. 24, 1984; revision received Jan. 27, 1985. Copyright © American Institute of Aeronautics and Astronautics, Inc., 1985. All rights reserved.

\*Associate Professor, Institute of High Speed Mechanics.

†Associate Professor, Department of Mechanical Engineering.

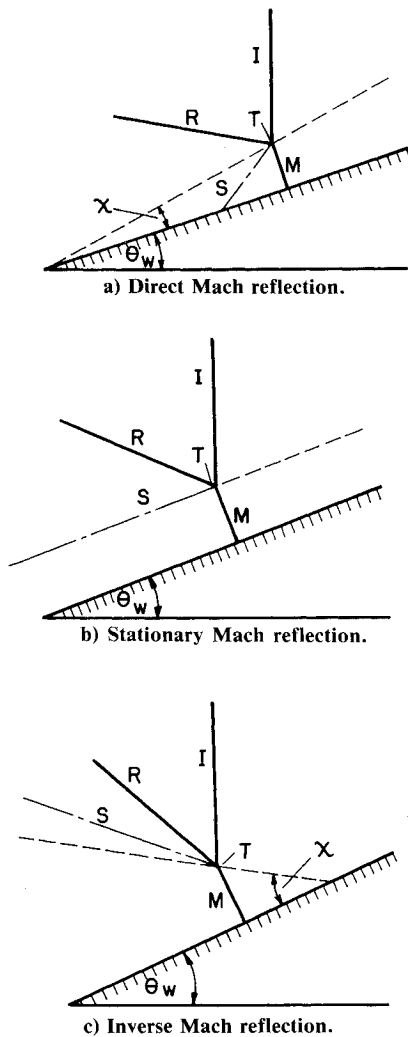


Fig. 1 Three types of a single Mach reflection.

Figures 3a-3c illustrate the wave configurations as well as the streamlines of the flow going through the various shock waves of direct, stationary and inverse Mach reflections, respectively. The initial conditions for these figures are taken from Ref. 4. The flow Mach number is  $M_0 = 2$  and it flows from right to left in all three configurations. If we define a counterclockwise deflection as positive and a clockwise deflection as negative, then for the direct Mach reflection (Fig. 3a) the net flow deflection is  $+7$  deg ( $17-10$  deg), for the stationary Mach reflection (Fig. 3b)  $0$  deg ( $13-13$  deg), and for the inverse Mach reflection (Fig. 3c)  $-3$  deg ( $8-11$  deg). Thus, one can differentiate between the three types of Mach reflection according to the net flow deflection across the incident  $I$  and reflected  $R$  shock waves, i.e.,

$$\begin{aligned} \theta_{\text{net}} = \theta_1 - \theta_2 = \theta_3 > 0 & \quad \text{direct Mach reflection} \\ = 0 & \quad \text{stationary Mach reflection} \\ < 0 & \quad \text{inverse Mach reflection} \end{aligned}$$

The  $(P, \theta)$  shock polar is often used to illustrate the shock wave reflection phenomena from yet another perspective.<sup>5-7</sup> Consider Fig. 4 in which three different combinations of  $I$ - $R$  shock polars are illustrated. The  $I$  polar corresponds to the incident flow Mach number  $M_0$  (see Fig. 3) and hence is identical for the three types of Mach reflection shown in Fig. 3.  $R_I$ ,  $R_{II}$ , and  $R_{III}$  are the shock polars for the flow in states 1 of the direct, stationary, and inverse Mach reflections, respec-

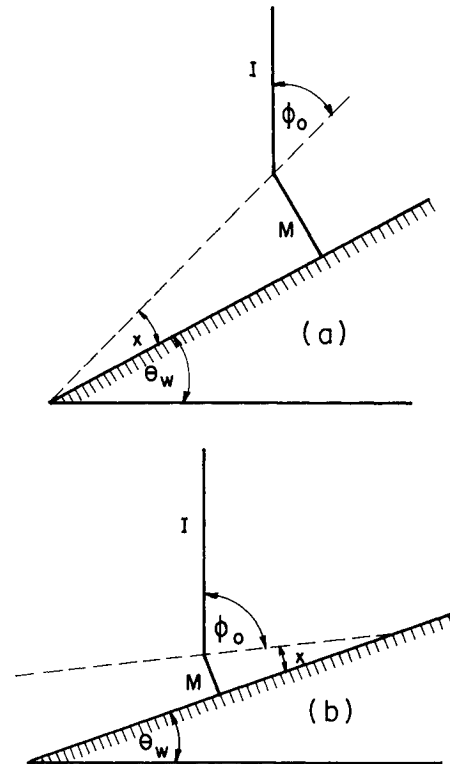


Fig. 2 Definitions of the angle of incidence  $\phi_0$  and the triple-point trajectory angle  $\chi$  in a) a direct Mach reflection and b) an inverse Mach reflection.

tively. The intersection of the  $R$  polar with the  $I$  polar yields a possible Mach reflection. The intersection point represents states 2, (behind the reflected shock wave  $R$ ) and 3 (behind the Mach stem  $M$ ) of a Mach reflection. These two states, which are thermodynamically different, coincide on the  $(P, \theta)$  plane to one single point because they are separated by a slipstream across which there is no pressure change ( $P_2 = P_3$ ) and along which the flows are parallel on both sides ( $\theta_1 - \theta_2 = \theta_3$ ).

The three different  $I$ - $R$  polar combinations of Fig. 4 represent the three different types of Mach reflection shown in Fig. 3. The intersection of the  $I$ - $R_I$  polars (point a) results in a positive net deflection, i.e.,  $\theta_{\text{net}} = 7$  deg  $> 0$ . Consequently, the intersection of the  $I$ - $R_I$  polars (at point a) corresponds to a direct Mach reflection. For the  $I$ - $R_{II}$  polar combination, however, the net deflection is zero,  $\theta_{\text{net}} = 0$ . Therefore, the intersection of the  $I$ - $R_{II}$  polars (at point b) represents a stationary Mach reflection. The  $I$ - $R_{III}$  polars represent yet another situation. In this case, the deflection of the flow by the incident shock wave  $R$  is greater than the deflection by the incident shock wave  $I$ , resulting in a negative net deflection,  $\theta_{\text{net}} = -3$  deg  $< 0$ , which can be obtained only through an inverse Mach reflection.

It is well known that the intersection of any  $R$  polar with the  $P$  axis represents a possible solution for a regular reflection. Consequently, the  $I$ - $R_{II}$  polar intersection occurring exactly on the  $P$  axis also represents a possible regular reflection. This possible regular reflection can be clearly seen in Fig. 3b if one removes the flowfield in the region below the slipstream and replaces it by a plane wall.

In all the  $I$ - $R$  combinations; which are similar to the  $I$ - $R_{III}$  combination of Fig. 4, both an inverse Mach reflection (at point c) and a regular reflection (at point d) are possible. However, it is an experimental fact that in both steady and pseudosteady flows, the regular reflection at point d is the reflection that occurs. As a matter of fact, as will be shown subsequently, the inverse Mach reflection is possible only in truly unsteady flows.

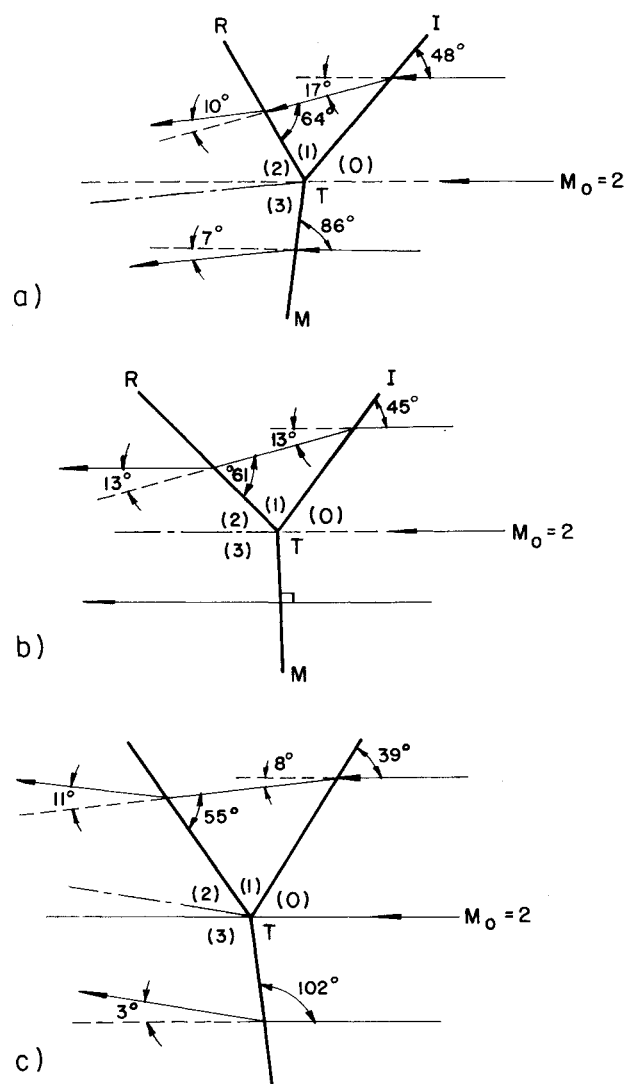


Fig. 3 Schematic illustration of the flow streamlines through a) a direct Mach reflection, b) a stationary Mach reflection, and c) an inverse Mach reflection.

### Experimental Facility and Technique

The experiments were conducted on the Institute of High Speed Mechanics 6 × 15 cm pressure driven shock tube.

The shock wave velocity was measured with pressure transducers (Kistler model 606), an Iwatsu UC 7641 digital counter, and an Iwatsu DM 901 recorder. The pressure transducers were mounted 120 mm apart just ahead of the test section. The effects of attenuation and acceleration of the shock wave were checked in the preparatory experiments. They were found to be negligibly small.

Dry air at initial pressures of  $3 < P_0 < 150$  Torr was used as the test gas. The initial temperature  $T_0$  throughout the experimental investigation was about 300 K.

The nonstationary phenomenon was recorded using interferometry and shadowgraph methods. A giant-pulse ruby laser (6943 Å) with a 20 ns light pulse width was used as a light source to obtain the instantaneous (single-shot) photographs. For the continuous observation of the shock diffraction process an Imacon high-speed camera (John Hadland Model 700) was used in both the framing and streak modes.

### Transition from Mach to Regular Reflection over Cylindrical Concave Wedges

When a planar shock wave collides with a cylindrical concave wedge in a shock tube, it reflects initially as a Mach reflection. As the incident shock wave propagates along the

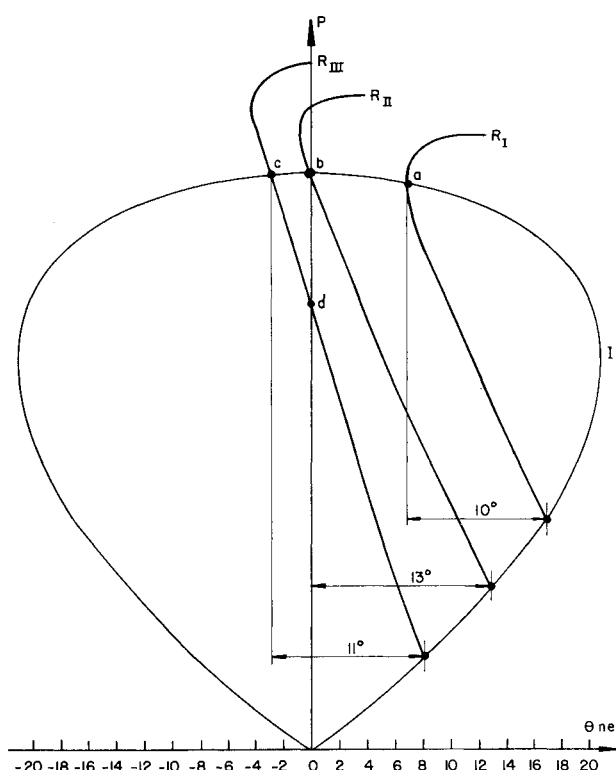


Fig. 4 Three *I-R* polar combinations illustrating a direct Mach reflection at point a, a stationary Mach reflection at point b, an inverse Mach reflection at point c, and a regular reflection at point d.

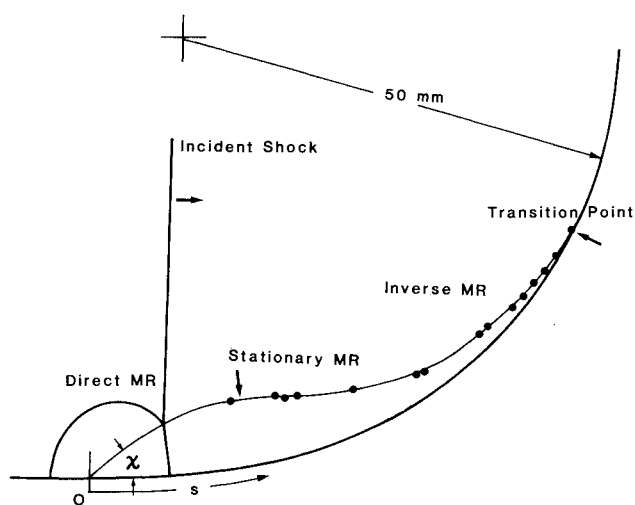
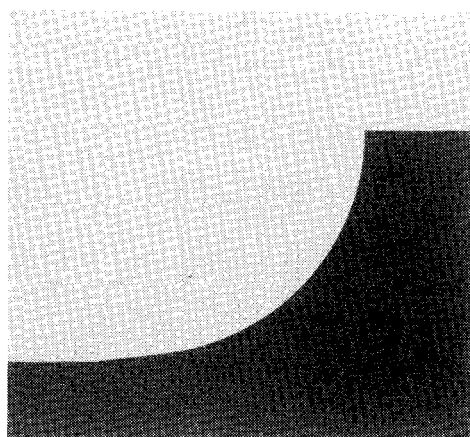


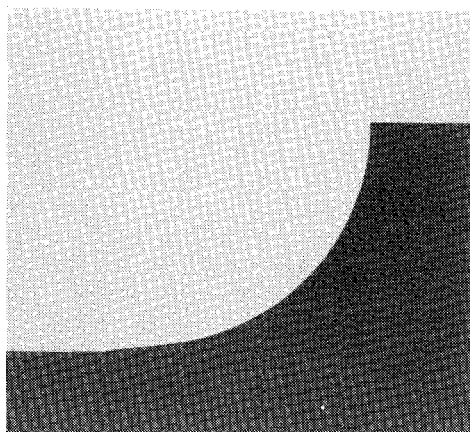
Fig. 5 Triple-point trajectory over a concave cylindrical wedge.

concave surface, a transition from Mach to regular reflection occurs.<sup>8</sup> An analytical criterion for this transition from Mach to regular reflection is still unavailable. During the course of our investigation and search for this criterion, the triple-point trajectory was studied. A typical trajectory is shown in Fig. 5. Inspection of this figure indicates that the triple-point trajectory can be divided into two parts: 1) a part along which the Mach stem is growing, i.e.,  $d\lambda/dS > 0$ ; and 2) a part along which the length of the Mach stem decreases, i.e.,  $d\lambda/dS < 0$ , until it vanishes at the transition point  $\lambda = 0$ . Thus, there is one single point along the triple-point trajectory at which  $d\lambda/dS = 0$ .

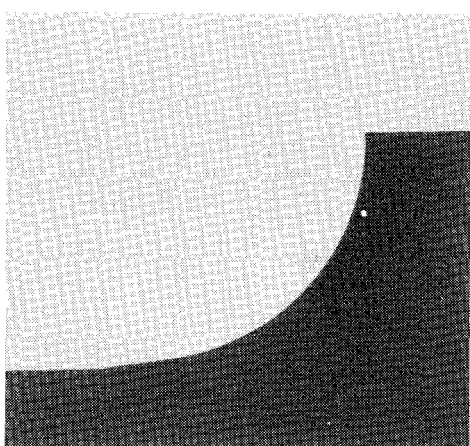
Recalling the foregoing discussion concerning the differences between various types of Mach reflections suggests that this transition process goes through the following sequence of events. First, a direct Mach reflection along the part where  $d\lambda/dS > 0$ . Then at the point where  $d\lambda/dS = 0$ , a



a) Direct Mach reflection.



b) Stationary Mach reflection.

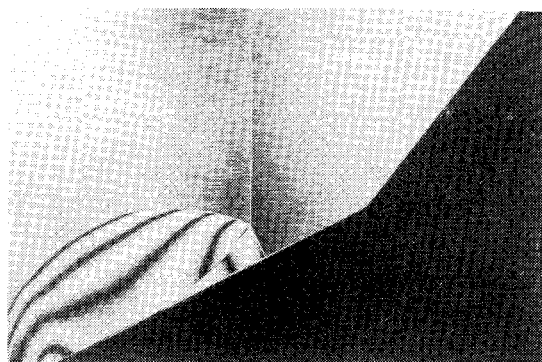


c) Inverse Mach reflection.

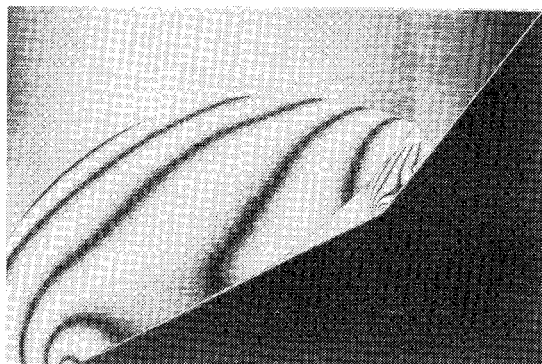
Fig. 6 Shadowgraphs of Mach reflections over a concave cylindrical wedge.

momentary stationary Mach reflection exists. Past this point, along the path where  $d\lambda/dS < 0$ , the inverse Mach reflection takes place. Finally, transition to regular reflection occurs at the point where the Mach stem vanishes ( $\lambda = 0$ ). Shadowgraphs illustrating these three different types of Mach reflection are shown in Fig. 6.

It will be shown subsequently that the regular reflection obtained after transition is part of a more complicated reflection, that of an inverse Mach reflection from the solid surface toward which it propagated and with which it eventually collided. Before we proceed to discuss the reflection of the inverse Mach reflection, one more type of shock wave phenomenon in which the inverse Mach reflection can occur will be illustrated.



a) Primary single Mach reflection (direct) over the first wedge.



b) Secondary single Mach reflection (direct) of the Mach stem of the primary single Mach reflection over the second wedge.

Fig. 7 Interferograms illustrating the reflection of a planar shock wave over a double-wedge model.

### Reflection of a Planar Shock Wave over a Double Wedge

The double-wedge reflection is another phenomenon in which an inverse Mach reflection can occur. In this phenomenon, the incident shock wave is reflected over two successive wedges. Initially, the incident shock reflects over the first wedge. Depending upon the shock wave Mach number  $M_i$  and the first wedge angle  $\theta_{w1}$ , a direct Mach reflection (single, complex, or double) or a regular reflection can occur. (See Refs. 5, 6, 9 and 10 for details.) Let us suppose that a Mach reflection has occurred and that the Mach stem of this Mach reflection encounters a second wedge  $\theta_{w2}$  in such a way that it reflects from the second wedge also as a direct Mach reflection. As time passes, these two Mach reflections (the primary and the secondary) must interact. Since the nature of this interaction has not been investigated thus far, an experimental study of this phenomenon was conducted.

Figure 7a shows the primary direct Mach reflection over the first wedge. When the Mach stem of this Mach reflection collides with the second wedge, a secondary direct Mach reflection is obtained, as shown in Fig. 7b.

Figure 8 is a schematic drawing of the wave configuration shown in Fig. 7b. Two triple points  $T_1$  and  $T_2$  are seen in Fig. 8. Three shock waves (incident  $I$ , reflected  $R$ , and Mach stem  $M$ ) as well as one slipstream  $S$  are associated with each triple point. The Mach stem of the first triple point  $M_1$  is the incident shock wave  $I_2$  of the second triple point. From the values of the incident shock wave Mach number  $M_{s1}$  and the first wedge angle  $\theta_{w1}$ , the values of the first triple-point trajectory angle  $\chi_1$  and the strength of the Mach stem  $M_{s2}$  can be calculated.<sup>5</sup> Then, by using the calculated Mach number of the first Mach stem  $M_{s2}$  and the value of the second wedge  $\theta_{w2}$ , the second triple-point trajectory angle  $\chi_2$  can be obtained. Thus, the two triple-point trajectories can be drawn as in Fig. 8. At point  $P$ , where the two trajectories intersect, the two triple points  $T_1$  and  $T_2$  join to form a new triple point. Our experimental study revealed that, depending upon the values of

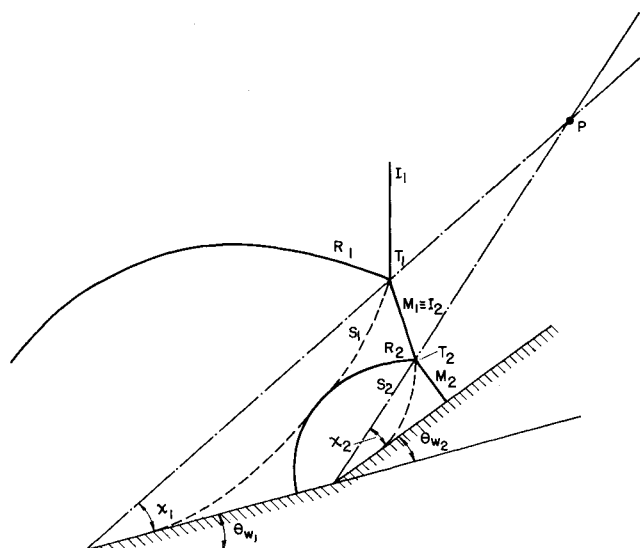


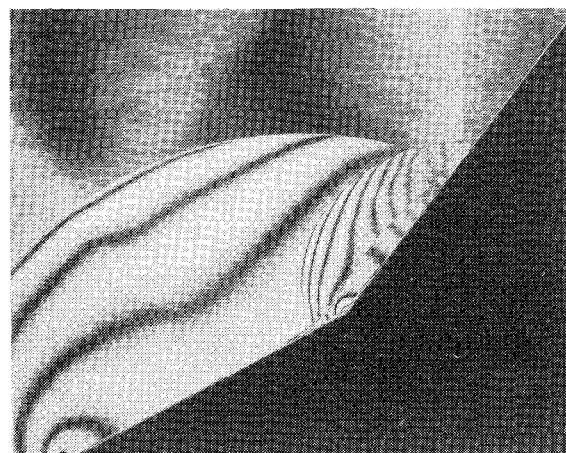
Fig. 8 Schematic illustration of the wave configuration shown in Fig. 7b.

$\theta_{w1}$ ,  $\theta_{w2}$ , and  $M_{s1}$ , this new triple point can move away from, parallel to, or toward the wedge surface, giving rise to a direct, stationary, or an inverse Mach reflection, respectively. These three different types of Mach reflection are shown in Figs. 9a-9c, respectively. Note that in all these three-shock configurations, the two reflected shock waves interact to form yet another triple point in which  $R_1$  plays the role of the incident shock wave.

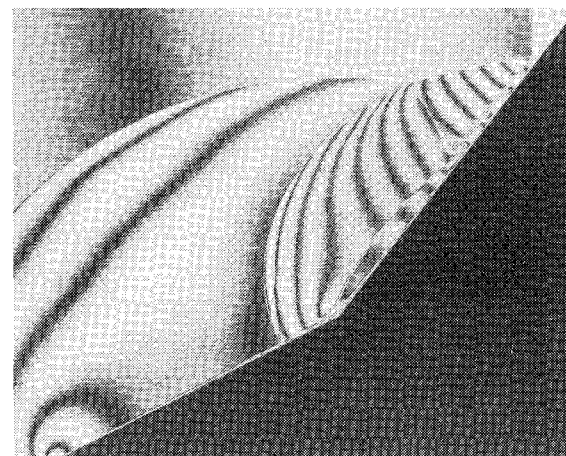
Before proceeding, it is important to note that, to the best of our knowledge, this is the first time that stationary and inverse Mach reflections over straight wedges were obtained in shock tube experiments.

### Reflection of the Inverse Mach Reflection

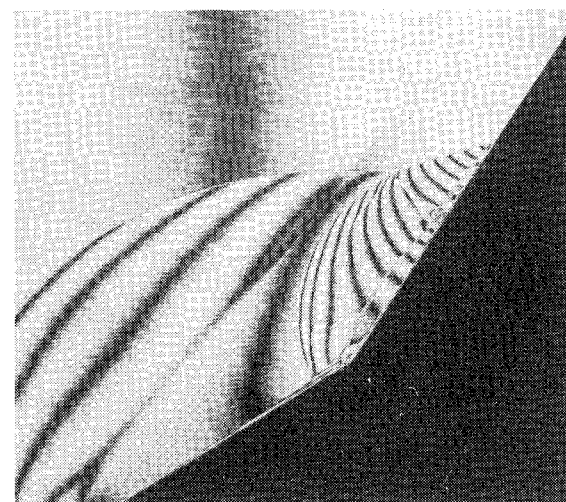
Since in an inverse Mach reflection the triple-point propagates toward the wedge surface, the inverse Mach reflection possesses a very unique feature, namely, its reflection from the surface. Figure 10a is a shadowgraph showing the wave configuration obtained after the inverse Mach reflection of Fig. 6c collided with the solid wedge surface and reflected from it. Figure 10b is an interferogram showing the wave configuration obtained after the inverse Mach reflection of Fig. 9c reflected from the solid surface. Figure 11 is a schematic illustration showing the dynamics of this reflection. Figure 11a shows an inverse Mach reflection moving toward the wedge surface. Figure 11b illustrates the wave configuration at the exact moment when the triple point  $T$  collides with the wedge. The Mach stem  $M$  vanishes and the incident  $I$  and reflected  $R$  shock waves intersect on the wedge surface. The wave configuration of the reflected inverse Mach reflection is shown in Fig. 11c. The major result of the reflection of an inverse Mach reflection is a regular reflection ( $I$  and  $R$  meet along the wedge). However, a new triple point  $T^*$  is formed on the reflected shock wave. The nature of this triple point is yet to be investigated. The answer to the question of whether it is a new triple point or a reflection of the original triple point (Fig. 11a) is unclear. As can be seen in Fig. 11c, a shock wave connects this triple point with the wedge surface in such a way that it is perpendicular to the wedge (i.e., it does not reflect from the wedge). The slipstream (dashed line in Fig. 11c) of the triple point  $T^*$  is directed toward the wedge surface. Upon meeting the wedge surface, it reflects in a way that can be termed as a regular reflection of a slipstream. Note that the wave configuration shown in Fig. 11c can be clearly seen in both Figs. 10a and 10b. To the best of our knowledge, this reflection process, as well as the wave configuration resulting from the reflection of an inverse Mach reflection, have never been published before.



a) Direct Mach reflection.



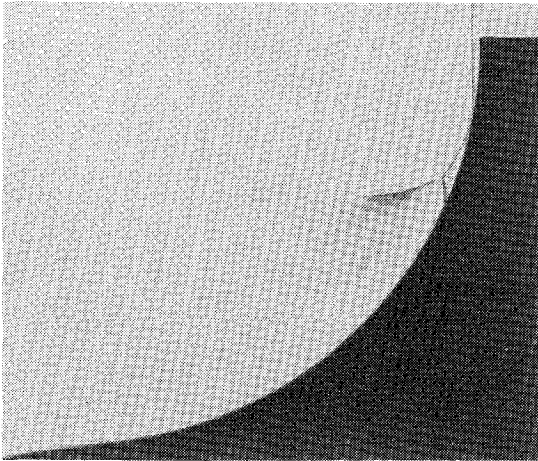
b) Stationary Mach reflection.



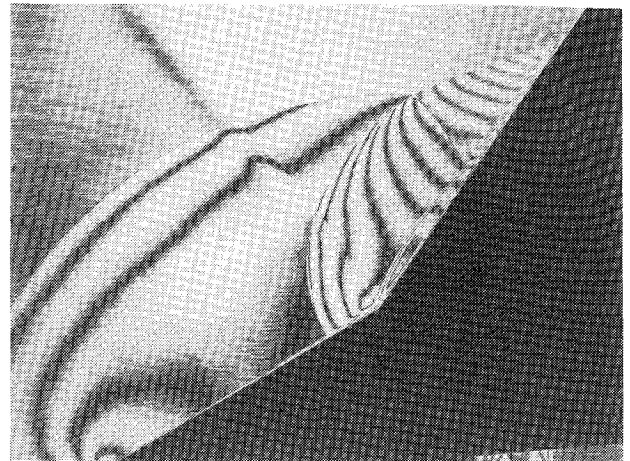
c) Inverse Mach reflection.

Fig. 9 Three interferograms showing the resultant reflection after the interaction of the two triple points ( $T_1$  and  $T_2$ ) of Fig. 8 at point  $P$ .

The wave configuration following the termination of an inverse Mach reflection can easily be explained using the  $(P, \theta)$  shock polar shown in Fig. 4. Assume that just before transition an inverse Mach reflection existed at the point where the  $R_{III}$  polar intersects the  $I$  polar (point c). Since the collision with the wall surface results in a regular reflection, it is obvious that this regular reflection must be at the point where the  $R_{III}$  polar intersects the  $P$  axis (point d). Consequently, one can clearly see that the transition from an inverse Mach to a

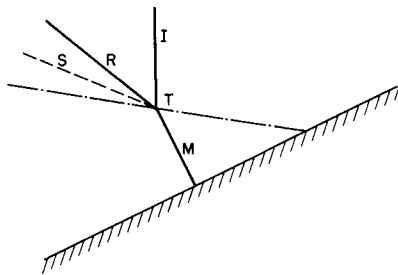


a) Reflection of the inverse Mach reflection shown in Fig. 6c.

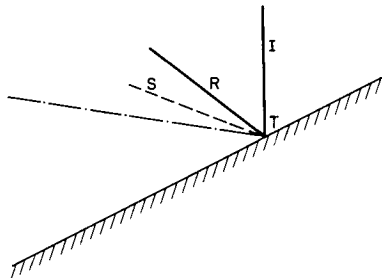


b) Reflection of the inverse Mach reflection shown in Fig. 9c.

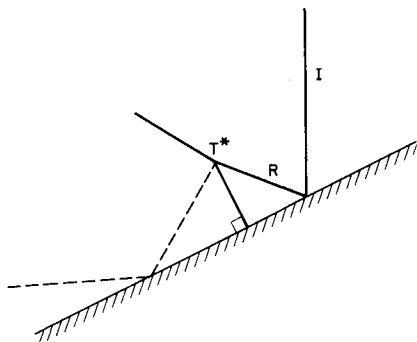
Fig. 10 Wave configuration obtained after the reflection of an inverse Mach reflection from the wedge surface.



a) An inverse Mach reflection propagating toward the wedge surface.



b) The inverse Mach reflection exactly at the moment when its triple point collides with the wedge surface.



c) The resultant regular reflection after the termination of the inverse Mach reflection and the normal shock wave following it.

Fig. 11 Schematic wave configurations illustrating the reflection of an inverse Mach reflection from a plane surface.

regular reflection is accompanied by a strong pressure decrease from  $P_c$  to  $P_d$ . This sudden pressure change can be supported only by a shock wave. Thus, the normal shock wave emanating from the triple point  $T^*$  (Fig. 11c) is probably responsible for supporting this sudden pressure change. Consequently, its strength must be very close to  $P_c/P_d$ . It should be mentioned that this normal shock wave was hypothesized

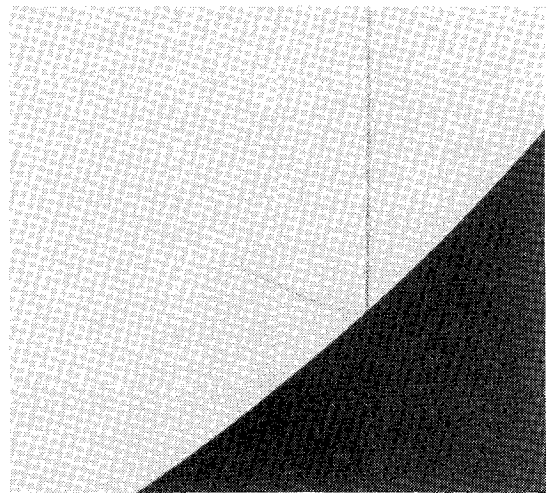


Fig. 12 A direct shadowgraph of a regular reflection obtained after the termination of a weak inverse Mach reflection.

by Henderson and Lozzi,<sup>12</sup> who said that "a system which develops a pressure discontinuity during transition cannot be in mechanical equilibrium." Furthermore, they said that "if a discontinuity occurs during transition then an unsteady wave of finite amplitude or a finite band of waves will be generated in the flow. These would be expansion [waves] for regular to Mach reflection transition and compression [waves] for Mach to regular reflection transition." The present experimental study partly verifies Henderson and Lozzi's hypothesis. Instead of a band of compression waves, a single shock wave appears. The formation of a slipstream at the triple point  $T^*$  where the three shock waves intersect is self-explanatory.<sup>3</sup>

It is also interesting to note that when the incident shock wave  $I$  is weak, the slipstream emanating from the triple point  $T^*$  becomes invisible. Figure 12 illustrates such a case very clearly.

## Conclusions

Motivated by the fact that in recent experimental investigations the inverse Mach reflection was observed, it was decided to investigate this special type of Mach reflection.

The differences between the three different types—direct, stationary, and inverse Mach reflections—were shown and discussed. Experimental evidences for the existence of the inverse Mach reflection in shock tube flows over straight and concave wedges were presented. To the best of our knowledge, this is the first time that inverse Mach reflections have been observed in two-dimensional flows in shock tube experiments.



The reflection process of the inverse Mach reflection was investigated. It has been shown that the termination of an inverse Mach reflection is followed by the formation of a special wave configuration of which the regular reflection is a major part. To the best of our knowledge, the present study of the reflection process of an inverse Mach reflection is the first of its kind. Furthermore, the wave configuration following the regular reflection (which is obtained after the termination of the inverse Mach reflection) was physically explained using the  $(P, \theta)$  shock polars.

In the course of the present study, a powerful experimental method for determining the transition phenomena<sup>11</sup>—namely, streak photography—was applied in order to positively verify the existence of an inverse Mach reflection as well as its termination and transition to regular reflection.

### Acknowledgment

The authors would like to express their appreciation to Prof. M. Honda of the Institute of High Speed Mechanics, Tohoku University, Sendai, Japan.

### References

- <sup>1</sup>Mach, E., "Über einige mechanische Wirkungen des electrischen Funkens," *Akademie der Wissenschaften Wien*, Vol. 77, No. II, 1878, p. 819.
- <sup>2</sup>Takayama, K. and Ben-Dor, G., "A Reconsideration of the Hysteresis Phenomenon in the Regular  $\Rightarrow$  Mach Reflection Transition in Truly Nonstationary Flows," *Israel Journal of Technology*, Vol. 21, 1983, pp. 197-204.
- <sup>3</sup>Courant, R. and Friedrichs, K.O., *Supersonic Flow and Shock Waves*, Vol. 1, Interscience Publications, Inc., New York, London, 1948.
- <sup>4</sup>Oppenheim, A.K., Smolen, J.J., Kwak, O., and Urtiev, P.A., "On the Dynamics of Shock Intersections," *Proceedings of the 5th Symposium (International) on Detonation*, Office of Naval Research, Department of the Navy, Arlington, VA, 1970, pp. 119-135.
- <sup>5</sup>Ben-Dor, G., "Regions and Transitions of Nonstationary Oblique Shock Wave Diffractions in Perfect and Imperfect Gases," *UTIAS Rept.* 232, 1978.
- <sup>6</sup>Henderson, L.F., "On the Confluence of Three Shock Waves in a Perfect Gas," *The Aeronautical Quarterly*, Vol. XV, Pt. 2, 1964, pp. 181-197.
- <sup>7</sup>Kawamura, R. and Saito, H., "Reflection of Shock Waves: I. Pseudo-Stationary Case," *Journal of the Physical Society of Japan*, Vol. 11, No. 5, 1956, p. 584.
- <sup>8</sup>Ben-Dor, G., Takayama, K., and Kawauchi, T., "The Transition from Regular to Mach Reflection and from Mach to Regular Reflection in Truly Non-Stationary Flows," *Journal of Fluid Mechanics*, Vol. 100, Pt. 1, 1980, pp. 147-160.
- <sup>9</sup>Ben-Dor, G. and Glass, I.I., "Domains and Boundaries of Non-Stationary Oblique Shock Wave Reflections: 1. Diatomic Gas," *Journal of Fluid Mechanics*, Vol. 92, Pt. 3, 1979, pp. 459-496.
- <sup>10</sup>Ben-Dor, G. and Glass, I.I., "Domains and Boundaries of Non-Stationary Oblique Shock Wave Reflections: 2. Monatomic Gas," *Journal of Fluid Mechanics*, Vol. 96, Pt. 4, 1980, pp. 735-756.
- <sup>11</sup>Ben-Dor, G. and Takayama, K., "Streak Camera Photography with Curved Slits for the Precise Determination of Shock Wave Transition Phenomena," *Canadian Aeronautics and Space Journal*, Vol. 27, No. 2, 1981, pp. 128-134.
- <sup>12</sup>Henderson, L.F. and Lozzi, A., "Experiments of Transition of Mach Reflection," *Journal of Fluid Mechanics*, Vol. 68, Pt. 1, 1975, pp. 139-155.

## *From the AIAA Progress in Astronautics and Aeronautics Series*

### **RAREFIED GAS DYNAMICS—v. 74 (Parts I and II)**

Edited by Sam S. Fisher, University of Virginia

The field of rarefied gas dynamics encompasses a diverse variety of research that is unified through the fact that all such research relates to molecular-kinetic processes which occur in gases. Activities within this field include studies of (a) molecule-surface interactions, (b) molecule-molecule interactions (including relaxation processes, phase-change kinetics, etc.), (c) kinetic-theory modeling, (d) Monte-Carlo simulations of molecular flows, (e) the molecular kinetics of species, isotope, and particle separating gas flows, (f) energy-relaxation, phase-change, and ionization processes in gases, (g) molecular beam techniques, and (h) low-density aerodynamics, to name the major ones.

This field, having always been strongly international in its makeup, had its beginnings in the early development of the kinetic theory of gases, the production of high vacuums, the generation of molecular beams, and studies of gas-surface interactions. A principal factor eventually solidifying the field was the need, beginning approximately twenty years ago, to develop a basis for predicting the aerodynamics of space vehicles passing through the upper reaches of planetary atmospheres. That factor has continued to be important, although to a decreasing extent; its importance may well increase again, now that the USA Space Shuttle vehicle is approaching operating status.

A second significant force behind work in this field is the strong commitment on the part of several nations to develop better means for enriching uranium for use as a fuel in power reactors. A third factor, and one which surely will be of long term importance, is that fundamental developments within this field have resulted in several significant spinoffs. A major example in this respect is the development of the nozzle-type molecular beam, where such beams represent a powerful means for probing the fundamentals of physical and chemical interactions between molecules.

Within these volumes is offered an important sampling of rarefied gas dynamics research currently under way. The papers included have been selected on the basis of peer and editor review, and considerable effort has been expended to assure clarity and correctness.

*Published in 1981, 1224 pp., 6 × 9, illus., \$65.00 Mem., \$109.00 List*

TO ORDER WRITE: Publications Dept., AIAA, 1633 Broadway, New York, N.Y. 10019